

## MEASUREMENT OF SURFACE REACTIONS IN THE SPACE ENVIRONMENT

*Wedad A. Abdou and Lawrence R. Megill - Globesat, Inc.;*  
*David A. Brinza - Jet Propulsion Laboratory;*  
*Roger C. Hart and R. Gilbert Moore - Utah State University;*  
*J. Andrew Sexton - Sverdrup Corporation; and Ali Siahpush - EG&G*

Serious degradation is experienced by the external surfaces of spacecraft that operate in low earth orbits for extended periods of time, as a result of the ablative effects of atmospheric atomic oxygen, possibly catalyzed by solar ultraviolet radiation. Improved base materials and surface coatings are being developed by government, university and industry teams to combat the effects of this degradation.

A small spacecraft and a suite of associated instruments, designed to measure the performance of improved, atomic-oxygen-resistant materials and coatings in orbit and to telemeter the resulting data and video images to earth at intervals during a one-year mission, have been described in a definition study sponsored by the Langley Research Center under NASA's In-Space Technology Experiments Program.

Instruments selected for use in this miniature orbiting laboratory include a radio frequency mass spectrometer, a set of quartz crystal microbalances, a set of osmium-based atomic oxygen sensors, a scatterometer, a set of osmium actinometers and a scanning optical microscope. The design of these instruments and their use in the overall experiment are summarized in this paper.

### INTRODUCTION

Serious degradation is experienced by external surfaces of spacecraft that operate in low earth orbits for extended periods of time. Prior to the Space Shuttle era, solar ultraviolet radiation (UV) and thermal vacuum exposure were considered to be the major causes of that degradation. During the past several years, however, extensive theoretical and experimental investigations by NASA and university scientists, both in space and in the laboratory, have identified atomic oxygen (AO), possibly catalyzed by UV, as the principal contributor to the degradation process [1,2,3].

As a part of those investigations, short-term experiments were conducted during the STS-5 Space Shuttle mission in 1982 and the STS-8 mission in 1983, in which selected material specimens were exposed to ram flow on orbit, then were examined in the laboratory, post flight, to determine the degree of specimen degradation that resulted from that exposure. For those experiments, AO concentrations in the flight environment were calculated by employing thermospheric models, with possible errors up to 25%. In order to reduce those errors, NASA plans to fly an extensive series of material samples and a co-located quadrupole RF mass spectrometer in a follow-on, short-term Shuttle experiment, referred to as the Evaluation of Oxygen Interaction with Materials, Third Series (EOIM-3), on the STS-44 mission in 1991 [4].

In addition, large numbers of test materials were placed in low earth orbit (LEO) in the Long Duration Exposure Facility (LDEF) on the STS 41-C mission of the Space Shuttle in April of 1984 [5]. This orbiting facility is scheduled to be retrieved in late 1989 and will yield a great deal of information on the integrated effects of exposure to the LEO environment on selected materials over a very long period of time.

Also, the Strategic Defense Initiative Organization (SDIO) is collecting a wide variety of exposure effects data from Sparta Corporation's "Space Materials Experiment," that was launched on the Delta 183 mission in March of 1989 [6]. This experiment is expected to return data for a period of three to nine months, depending on when on-board consumables, such as attitude control thruster fuels, are depleted.

What is needed now is a series of small, inexpensive spacecraft that can function as test beds for the evaluation of new structural materials, optical and thermal protective coatings and the like, as they are developed for use on the Space Station Freedom, on its co-orbiting and polar-orbiting companions, and on various Department of Defense spacecraft that are designed to be placed in long-term, low-altitude orbits. These test beds can also serve to provide on-orbit verification of measurements performed in ground-based laboratory facilities that have been and will be established across the country to screen promising candidate materials.

Globesat, Inc., of Logan, Utah, assisted by Utah State University, has spent the past year in defining a low-cost spacecraft and a set of experiments designed to quantify the orbital environment in which low altitude spacecraft operate and to periodically measure the responses of materials exposed to that environment for a period of one year. This study, dubbed ATOMS for ATomic Oxygen Measurement Spacecraft, has been performed for the NASA Langley Research Center, under the auspices of NASA's In-Space Technology Experiments Program (INSTEP.) The present paper is a description of this definition study, together with an outline for developing the spacecraft and related instruments.

## EXPERIMENT OBJECTIVES AND SCOPE

The objectives of the experiment described herein are: to expose a series of material samples on the leading face of a small, three-axis-stabilized spacecraft in a circular orbit about the earth at an altitude of approximately 500 kilometers; to measure the responses of those samples to the orbital environment; to measure the characteristics of that environment; to transmit to earth at periodic intervals the data and images obtained from those measurements; and to analyze and evaluate the degradation and rates of degradation of the sample material surfaces that result from exposure to the measured orbital environment.

The instruments selected to accomplish those objectives are: a Radio Frequency Mass Spectrometer, for measuring ambient atmospheric gas densities; a series of Osmium-Based AO Sensors, for measuring AO fluences; a series of Quartz Crystal Microbalances, for measuring sample material ablation rates; a series of Osmium Actinometers, also for measuring material sample ablation rates; a Scatterometer, for measuring the change in material sample surface properties; and a Scanning Optical Microscope, for obtaining detailed images of the surfaces of the material samples over time.

A Globesat GS-50 spacecraft bus has been selected to house and provide technical support to this suite of instruments. The GS-50 is a right octagonal cylindrical structure containing not only the material samples and instruments listed above, but a body-mounted solar array, a battery supply, a command and control computer, an attitude control system, a UHF command receiver, a telemetry transmitter, associated antennas, and a support mechanism compatible with a Space Shuttle Get Away Special canister or any of various expendable launch vehicle payload attach rings.

## TECHNICAL DESCRIPTION OF THE EXPERIMENT

### 1. MEASUREMENT OF AO FLUX

Two instruments have been chosen for determining the flux of AO impinging on the face of the spacecraft that is held in the orbital ram direction and upon which the material samples are mounted: the first, is a mass spectrometer, which will provide a continuous monitor of changes in AO and other atmospheric constituent concentrations during the life of the experiment and therefore a means of improving on exposure calculations.

The second instrument, an osmium-based AO sensor, has only recently been developed and made available for this type of measurement. It is much more compact, much simpler to build and far less expensive than is any mass spectrometer. The mission described in this study will provide for the first time an opportunity to make a direct comparison between the measurements performed in orbit by a series of osmium-based sensors and measurements performed under identical conditions by a mass spectrometer.

#### RF Mass Spectrometer

There are many good commercial mass spectrometer designs on the market, most of which are sold in association with large, complex, laboratory analysis systems. Unfortunately, however, commercial suppliers are generally not interested in modifying their systems for use in the space environment, due to the limited market involved. Historically, therefore, space scientists have built their own mass analyzers, which are the crucial components required for space application, or subcontracted them to specialized suppliers of space-rated components. Most of these instruments, however, have been designed either for use in the "D" or "E" regions of the ionosphere, where the requirements on the spectrometers are much more severe than for orbiting instruments, or they have designed them for planetary missions, with attendant extremely high reliability requirements. As a result, most of these instruments are too large, require too much power,

and/or are priced too high for consideration in the program. It appears, therefore that the best way to obtain an instrument suited to the small spacecraft baselined for this study will be to build, in house, an RF mass spectrometer. A small linear accelerator is the critical element in the mass selector of this instrument, and the requirements on it for the present application are modest. At LEO altitudes, one needs only to distinguish the ratio of (AO) density to the densities of molecular nitrogen ( $N_2$ ) and molecular oxygen ( $O_2$ ). This requires a mass resolution of not greater than 10 or so. Spacing between accelerating electrodes will be maintained by utilizing ceramic spacers. The grid structure and filaments required in the ionizer will be constructed utilizing techniques employed in fabrication of electron accelerators by the Space Dynamics Laboratory of Utah State University. Several tens of such devices have been flown by the laboratory on a wide variety of launch vehicles over the last two decades, with good results. The ionizer will be calibrated by the university's Chemistry Department. A small capillary electron multiplier will be used as the final detector. Figure 1 shows the basic layout of the instrument. Neutral particles will be introduced into the ionizer chamber, which will be facing in the ram direction. The filament will produce electrons, which will be accelerated to about 100 eV, near the maximum of the ionization cross section. Utilizing a beam energy of this magnitude will produce reasonable fluxes of  $O^+$ . Calculations indicate that, with an ionizing current of 1 milliampere, one can expect to produce of the order of one million ions per second. With a transparency of the order of one thousandth for the mass selector, counting rates can be expected in the hundreds per second at mass peaks.

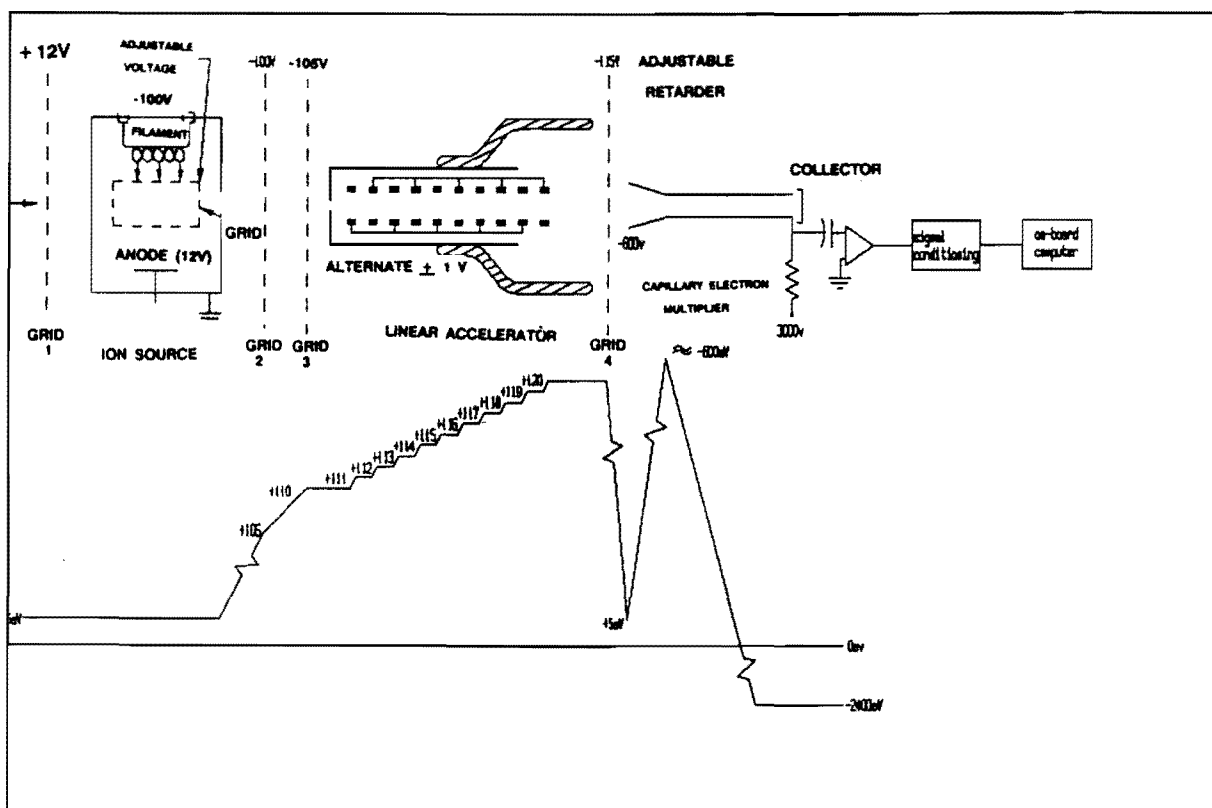


Figure 1: Layout of Boyd RF Mass Spectrometer with estimated electric potentials and energies of ions at various points along the instrument.

A beam energy of 100 eV will also dissociatively ionize some of the  $O_2$  present at that altitude; therefore, experiments will be conducted both in the laboratory and in space at energies below the 20 eV required to dissociatively ionize  $O_2$ . These experiments will produce very low counting rates but can be carried out for long periods of time and will give an indication of the errors involved in the use of the higher energy beam. The  $[O_2]/[O]$  ratio decreases rapidly in altitude, and, if the satellite is at a high enough altitude (above 300 km for most exospheric temperatures), this ratio will be considerably less than one.

After the neutrals are ionized, they are introduced into the linear accelerator section of the RF accelerator.

In this region, the velocity is kept large enough that the incremental velocity added between sections is small. This enables one to use a constant frequency between the sets of electrodes. This can be optimized, to some extent, by varying the spacing as the ions are accelerated, if the mass range being scanned is small; however, optimization will probably not be required for this application. The ions will acquire a few volts of additional energy only if the mass is correct for the frequency between the electrodes. For O, this frequency is 35.3 MHz, while, for O<sub>2</sub> and N<sub>2</sub>, the frequencies are 25.0 MHz and 26.7 MHz, respectively. The ions which exit the accelerator are discriminated by a retarding potential. Figure 1 illustrates the energy of the ion and the potential at various points across the instrument.

The surviving ions are then accelerated to several hundred volts in order to optimize secondary emission in the detector. The multiplier raises the current to a level at which they can be easily counted. A conventional discriminator and counter will be used to acquire the data. The data requirements for this instrument are modest. If a measurement is made every five minutes during the initial portions of the flight, and if three count measurements are made for each mass of interest, this results in 9 counts to 12 bit accuracy and 9 frequencies to 8 bit accuracy, resulting in 24 bytes per measurement, including a time record. Fewer than 7 kilobytes need to be transmitted per day from this instrument. The transmission time required, at the rate of 9600 baud, will thus be of the order of 6 seconds per day.

### Osmium-Based AO Sensor

Osmium is known to react efficiently with AO and to undergo significant mass loss when exposed to the space environment [7]. The mass loss is due to the formation of OsO<sub>4</sub>, which has a relatively high vapor pressure. The increase in electrical resistance of an osmium specimen exposed to ram flow in low earth orbit, as a result of its decrease in cross section, is a sensitive measure of the amount of AO present in the atmosphere at the altitude of the orbit. From the rate of the reaction, specimen orientation and exposure interval, the fluence and, hence, the number density of AO can be determined.

A simple, active sensing device for real-time measurement of AO flux, based on these principles, is under development by Dr. David Brinza and his associates at the Jet Propulsion Laboratory. Osmium thickness requirements for sensors with varying orbital lifetimes have been estimated with the aid of osmium erosion rates measured in an experiment on the Space Shuttle STS-8 mission [8]. In that case, an exposed sample lost approximately 1.1 microns in thickness during a 41-hour exposure period. The estimated AO fluence for this exposure was  $3.5 \times 10^{20}/\text{cm}^2$ ; hence, the apparent volume loss per incident atom is  $3.1 \times 10^{-25} \text{ cm}^3/\text{atom}$ . Using this value for osmium removal efficiency permits the prediction of the response of a particular sensor geometry to specified orbital conditions.

The choice of osmium metal for the simple resistive sensor was made in order to take advantage of the volatility of the oxide. As the osmium metal surface reacts with AO, under the low-pressure conditions existing in orbit, the oxidized metal sublimates away from the surface and continually exposes fresh metal to the environment. This feature overcomes one of the principal disadvantages of silver-based sensors, in which the oxide formed early in the exposure interval remains intact, and further oxidation is dependent on migration or diffusion of oxygen through the oxide layer. In addition, silver sensors are difficult to calibrate in terms of response to rapid changes in AO flux. Consideration was given to using a carbon-based sensor under development at the NASA Marshall Space Flight Center, but its temperature sensitivity and the effects of carbon film morphology on its response may cause significant problems in its calibration.

The chief problem in preparing osmium sensors in quantity for use in an AO measurement spacecraft is the difficulty of producing uniform films at thicknesses greater than 1000 Angstroms (A). Evaporated osmium films are no longer commercially produced, and, even when such films were commercially prepared, they had a tendency to crack at thicknesses greater than 500 A. Fortunately, an electrochemical method of deposition (plating) has been developed for this metal [9]. According to the published method, uncracked films with a thickness greater than 10,000 A have been deposited on gold-flashed cathodes. JPL's early attempts at plating osmium according to the described techniques have produced acceptable films on the order of 2000 A thickness, and they fully expect to achieve values of 10,000 A in the near future.

Each individual device is fabricated with four independent active sensing elements to permit redundancy of measurement (for improved statistics). Parallel devices will also be flown, with multiple thicknesses of erodable overcoatings applied, such that the individual elements become exposed sequentially and thus extend the lifetime of the devices. Some details for fabrication of the devices are as follows: Fused silica substrates (Heraeus-Americal TO-8 grade) with dimensions 1" x 1/2" x 1/16" are carefully cleaned to remove

foreign matter from the surface. The sensor element cathodic strips are prepared by evaporative deposition of first a very thin layer (20-50 Å) of titanium to improve adhesion followed by 100 Å of gold. Direct deposition of four 0.050" width strips, separated by 0.200" gaps, on each substrate is performed through a mask which holds eight substrates. A subsequent deposition of thicker (200 Å) gold strips is performed through a mask with slots perpendicular to the sensor strip orientation, in order to provide continuity for the osmium plating of the sensor elements. The devices are then plated as prescribed in the published method. The bonding pad areas are then formed by a thick gold deposition (2000 Å) through the same mask used to provide continuity for the electroplating. Teflon-coated 30 gauge wire is soldered to the bonding areas on either side of each strip. Finally, the individual sensor elements are electrically isolated by scraping the gold from the regions between the bonding pads for the leads. Each sensor strip is tested with a DVM to insure proper initial resistance values.

## 2. MEASUREMENT OF AO INTERACTION WITH SAMPLE SURFACES

There are two measurements of interest for evaluating the effect of the space environment on materials. One is the material ablation rate ( $\text{mg}/\text{cm}^2$ ), and the other is the change in optical properties, such as surface light-scattering characteristics. If AO fluence is known, and control of solar ultraviolet is taken into consideration, measurement of ablation rates will lead to the determination of reaction efficiencies of the ablated materials with AO. The change in surface scatter will result in a measure of surface roughness during the degradation process.

A Quartz Crystal Microbalance (QCM) and an Osmium Actinometer have been selected for measuring ablation rates for various materials, and a Scatterometer has been selected for measuring the surface roughness of various optical surfaces.

QCMs have been used in similar experiments on the STS-8 mission to determine the ablation rates and reaction efficiencies of several materials with AO. The osmium actinometer is a new technique that has been developed by JPL for measuring ablation rates, and the present experiment will be the first orbital use of this device. The Scatterometer is typically used in the laboratory to characterize optical surfaces and to evaluate their root mean square roughness.

### Quartz Crystal Microbalance

In its simplest form, a QCM consists of a thin quartz wafer, coated with a specimen material and attached to driving and counting electronics. The coated crystal is driven at high frequency (typically around 10 MHz); a change in the mass of the wafer by deposition or removal of its surface coating causes the frequency of oscillation to deviate from the driving frequency. The change in frequency is proportional to the mass change and is also dependent on the absolute temperature of the crystal; therefore, a second, identically coated crystal, shielded from the mass flux, is used in parallel with the first as a reference. As long as the two crystals have the same temperature, the absolute temperature dependence is removed, and the mass change is related to the beat frequency between the two crystals. Mass sensitivities as low as  $4.4 \times 10^{-9} \text{ g}/\text{cm}^2\text{-Hz}$  are specified for low-temperature operation.

The QCM is an established instrument for measuring deposition or removal of thin films, and several manufacturers have been identified as sources for a flight instrument. Little modification of the commercial QCM will be necessary, so incorporating it into the ATOMS suite of instruments will consist of identifying sample materials, coating the measuring crystal, mounting instruments in selected positions on the satellite, and designing the interface to the satellite's computer.

Preliminary selection of sample materials for the QCM experiment will be guided primarily by the considerations discussed later in this paper. Final selection will be determined by the ability to coat the quartz crystals with the desired materials, and by the maximum thickness of coating that can be applied. The sensor crystal will not oscillate properly when coated with a film greater than  $\sim 12$  microns in thickness.

Several types of QCM sensors are commercially available. Factors affecting selection of a flight instrument include size, packaging, thermal environment, and cost. To overcome the temperature dependence of the sensor crystal output, two matched crystals are used in each sensor head, one for detection of mass change, and a shielded one for reference. The two crystals are mounted in the sensor head, either in tandem or side by side, with the reference crystal protected behind a quartz window. When mounted in tandem, the

package is smaller and less expensive, but the reference crystal is not subject to the same thermal radiation as the sensor crystal and may reach a different temperature than the sensor crystal, causing errors in the measurements. When mounted side by side, the crystals will be in identical thermal environments. For that reason, this type of packaging will be most suitable for the project.

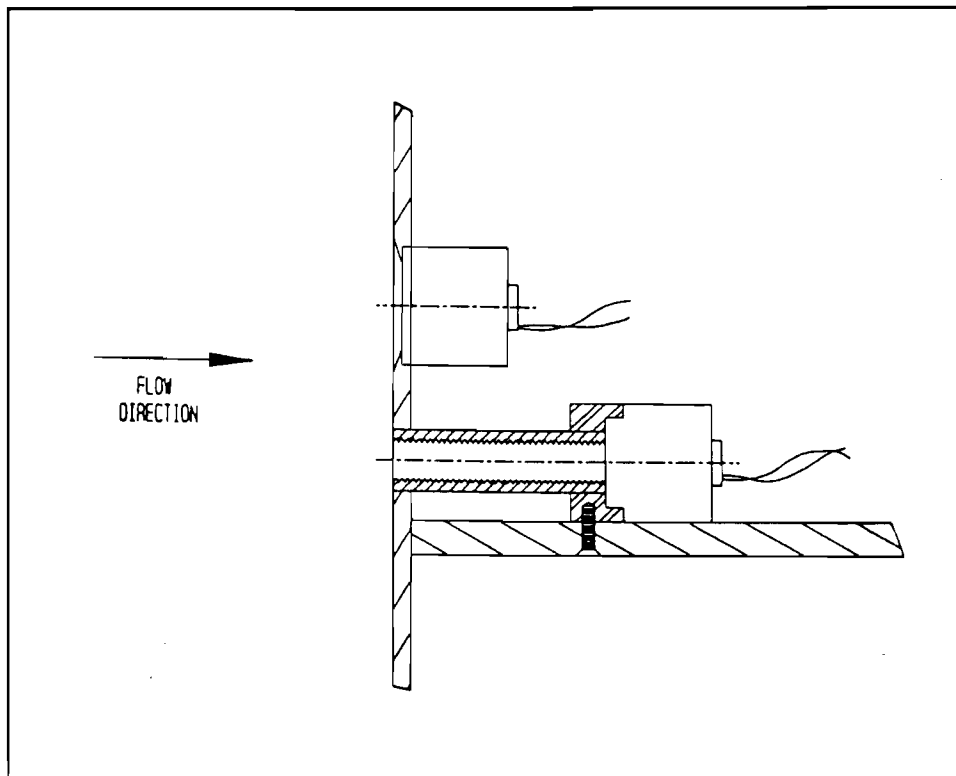


Figure 2: Optical baffle for UV-shielded QCM.

Results from the STS-8 mission indicate that ablation rates are possibly higher during sunlit periods than during eclipse. The validity of this observation can be evaluated by using the doublet QCM on the satellite surface in parallel with a second QCM, set in a recess behind an optical baffle, as shown in Figure 2, to reduce its exposure to solar UV, while still being exposed to the atmospheric mass flux. The field of view of the shielded QCM will be determined by the length and diameter of the baffle. By restricting the field of view to  $10^\circ$ , direct exposure to solar UV can be reduced from around 2000 hours per year to less than 80 hours per year.

A QCM will be placed inside the satellite shell to serve as a control sensor, and additional sensors will be placed on the satellite's wake face to observe mass changes, if any, in the anti-velocity direction. The QCMs will be thermally connected to the spacecraft shell and operated without active temperature control. The associated electronics will be a frequency counter, a circuit to read a resistive thermometer, and a power supply. By commutating the power and signal lines, any number of QCMs can be monitored with the same circuitry.

The frequency of measurements will be highest at the beginning of the mission; for example, once every day. Later, after ablation rates become well established, data may be acquired once every week, or even less frequently. Data storage and transmission requirements are modest and within the capabilities of the satellite subsystems.

An ablation model which predicts the behavior of materials in the low Earth orbital environment has been developed in a Ph.D. work which was supervised by the principal investigator [10]. This model will be our guide in the interpretation of the results obtained by the QCMs.

### Osmium Actinometer

As with the QCM, the Osmium Actinometer (Figure 3) will be used to measure the erosion or ablation rate of materials. The concept involved is different, however, and consists of initially coating the osmium

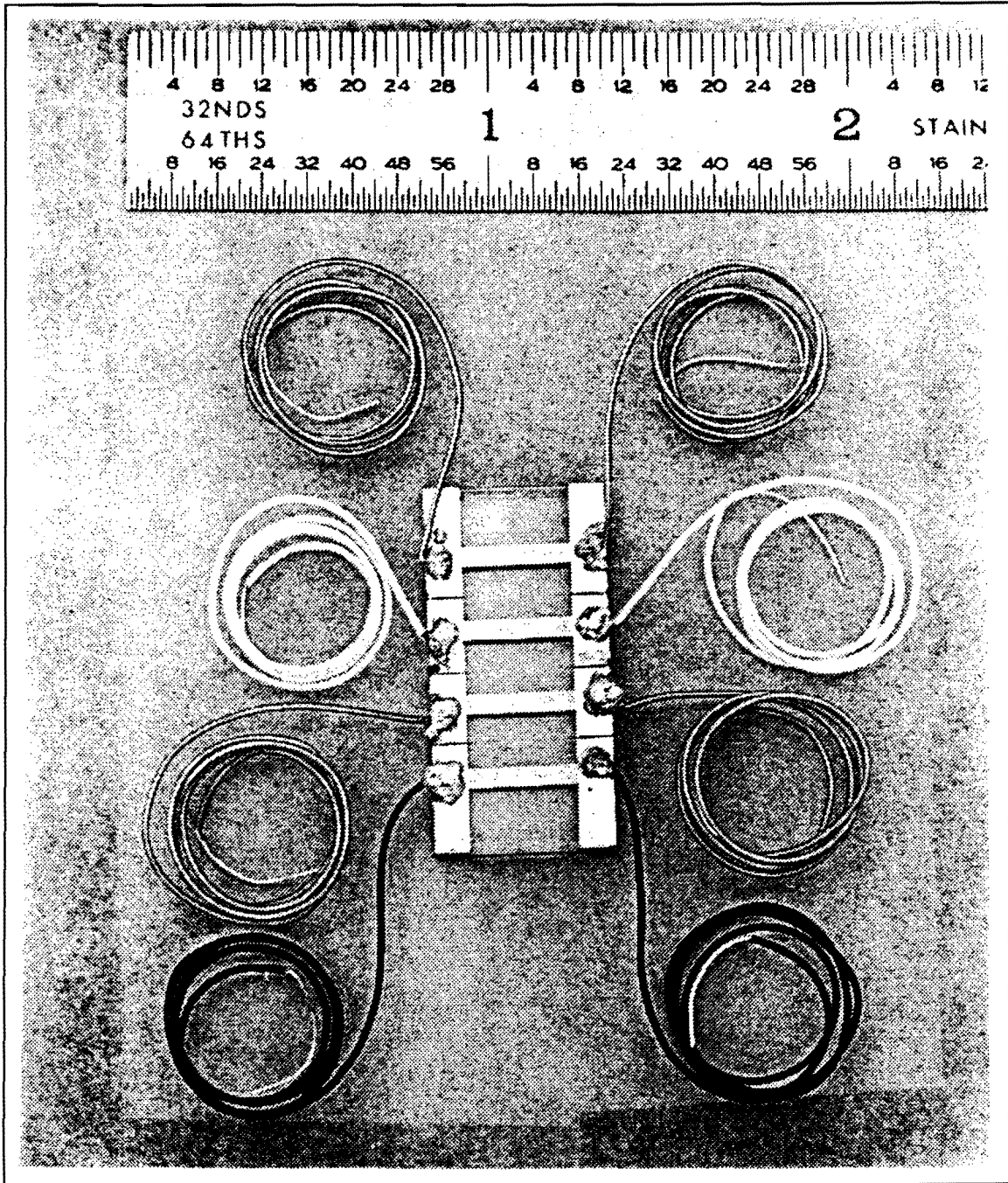


Figure 3: Osmium actinometer provided by JPL

with a film of the material under study, then observing the point at which the resistance of the osmium sensor begins to change. At this point, the specimen film has been completely eroded away. In order to extend the lifetime of this type of measurement, several parallel strips of osmium will be deposited on a 0.5" X 1" quartz substrate and subsequently coated with films of different thicknesses of the materials under investigation.

### Scatterometer

Light scatter has proven to be a sensitive measure of surface finish defects. When scatter is measured as a function of angle from the reflected specular beam, it is usually expressed in terms of the bidirectional reflectance distribution function or BRDF [11]. The BRDF is defined as the scattered surface radiance divided by the incident surface irradiance,

$$\text{BRDF} = \frac{(dP_s/d\omega_s)/(A \cos \theta_i)}{P_i/A} = \frac{dP_s/d\omega_s}{P_i \cos \theta_i}$$

where the incident surface irradiance is the light flux  $P_i$  (in watts) on the surface per unit of illuminated surface area ( $A$ ), and the scattered surface radiance is the light flux scattered ( $dP_s$ ) per unit surface area per unit projected solid angle ( $\omega_s$ ).

The value of BRDF is bidirectional, in that it depends on both the incident direction ( $\theta_i$ ) and the scatter direction ( $\theta_s$ ) and may be viewed as directional reflectance per unit steradian. Figure 4 illustrates the geometry used for the definition of BRDF.

BRDF measurements taken several degrees or more from the specular reflection with values above  $10^{-4} \text{ sr}^{-1}$  are relatively easy to make. For surfaces where the roughness height features are much less than a

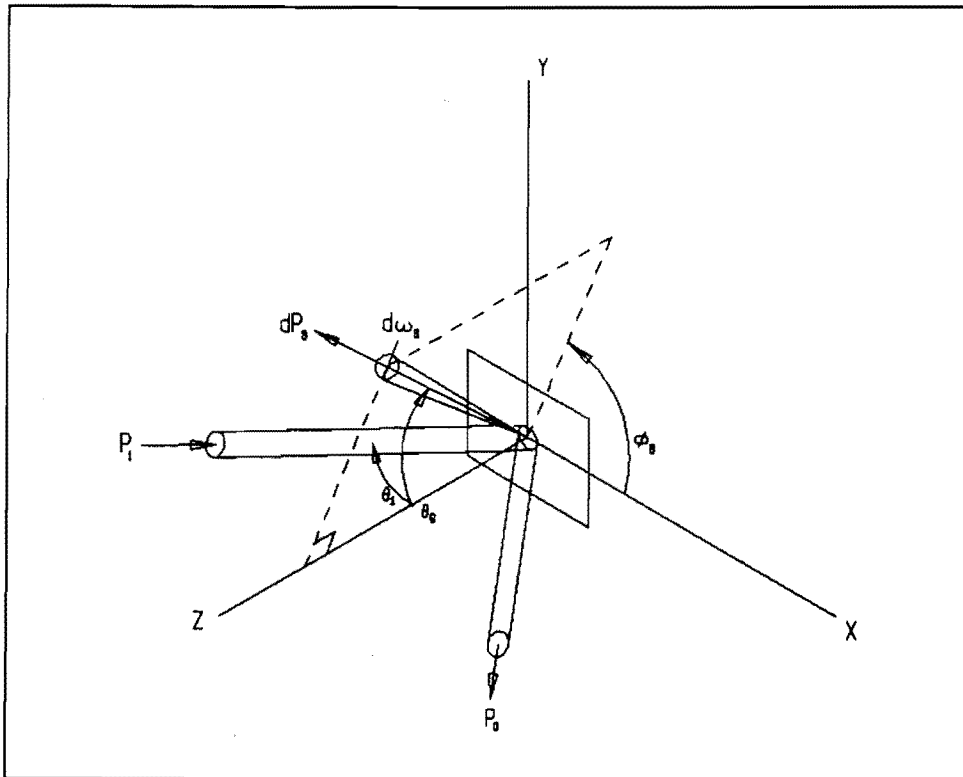


Figure 4: Geometry of scatter measurements.



wavelength of the scattering source, relationships have been developed, and proven, that allow the surface power spectral density (PSD) function to be calculated from the BRDF [11,12]. The PSD may be thought of as roughness power per unit roughness frequency. In this case, taking the integral of the power spectrum (its zeroth moment) gives the mean square roughness. Its second moment gives the mean square surface slope, and  $2\pi$  times the ratio of these moments gives the average surface wavelength. All of these quantities are limited to the bandwidths defined by the integration.

It is fairly common for straight line plots to be obtained when the PSD is plotted on a log-log scale [13]. This implies that the surface is fractal in nature; that is, surface structure appears more or less identical, regardless of the magnification through which it is viewed. It also means that the PSD can be expressed as a constant times a power of the inverse spatial frequency. The net result is that a great deal of surface information can be extracted from the measured BRDF of optically smooth reflectors.

Toomy, Mathis & Associates (TMA), Inc. of Bozeman, Montana, is a company which builds scatterometers and provides scatter measurement services to the public. To examine the sensitivity of their instrument in evaluating the degradation of surfaces in space, two samples of Kapton, one that flew on a Space Shuttle mission and one that served as a ground control for the flight sample, were sent to TMA for scatter measurements. The scatter data on these two samples, as shown in Figure 5, represent the change in BRDF with angle from the direction of specular reflection. The scatterometer was operated at a wavelength of 0.633 microns. The laser beam was incident at  $15^\circ$ , and a detector head was scanned in the plane of incidence through the specular reflection and the scattered light. The scattered light signal was then normalized by the incident power and plotted in BRDF format as normalized scattered light per unit solid angle (on a log scale) against detector angle from specular. During the scan, the detector crossed the light source and cut off the incident light, producing the dip shown at  $30^\circ$ .

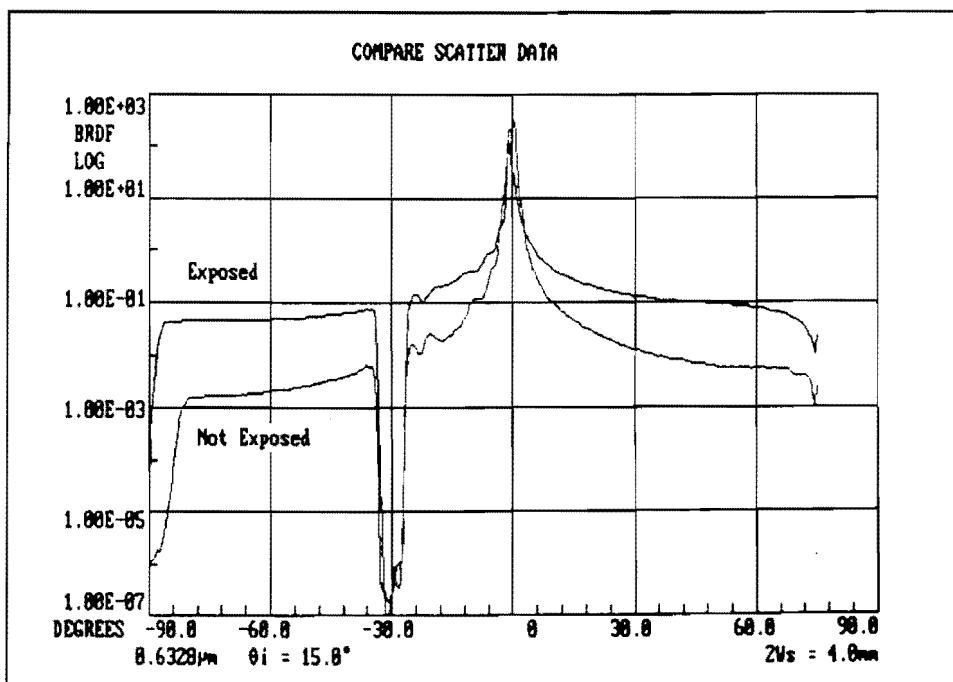


Figure 5: BRDF of kapton sample exposed to space on STS-8 flight compared with BRDF of ground control sample.

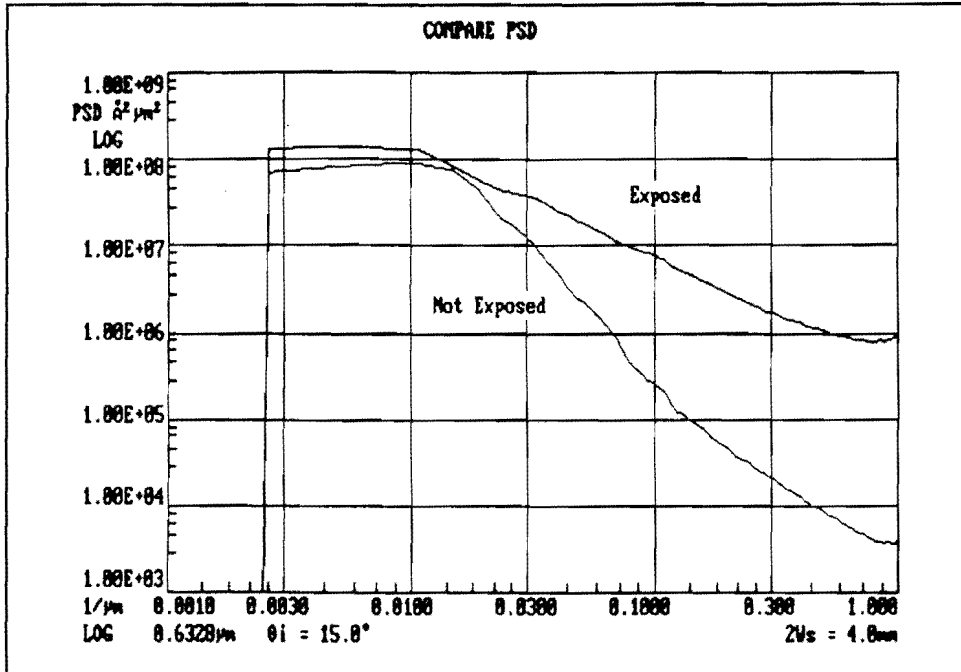


Figure 6: Power spectral densities (PSDs) for Kapton samples of Figure 5

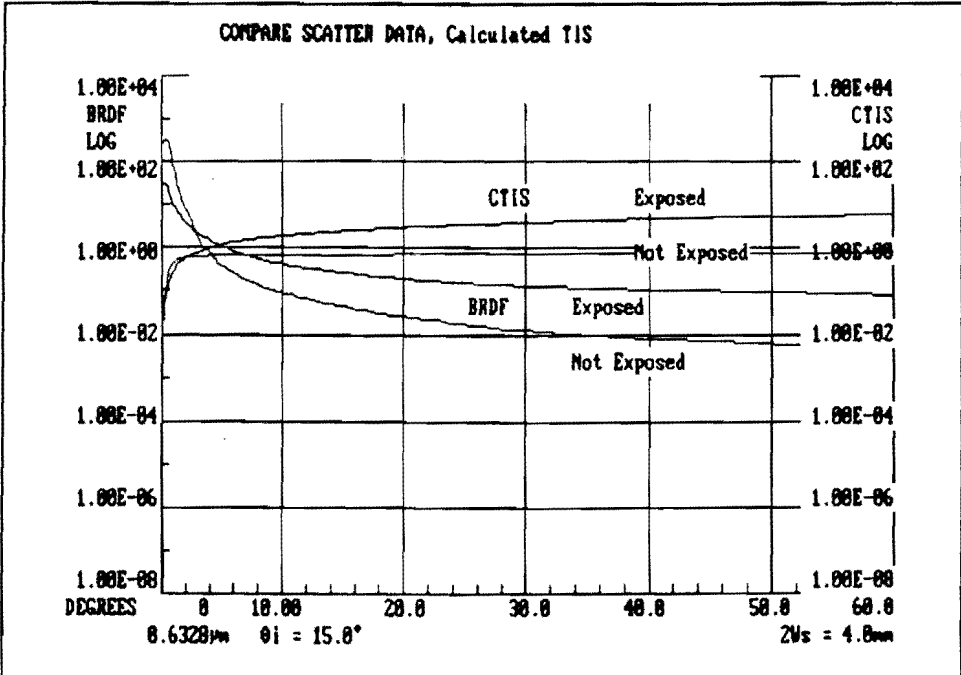


Figure 7: Calculated total integrated scatter for samples of Figure 5

The above results indicate two key points. First, as was expected, scatter measurements are a sensitive indication of surface change caused by exposure to the space environment, for both optically smooth surfaces and rougher materials. Secondly, the changes in the BRDF of these samples can be monitored at relatively large angles from specular. This is important, because it means that a relatively simple instrument can be designed for in situ measurement of space-based samples that will detect the expected changes in sample topography.

The exact design of the proposed scatterometer is proprietary and will not be given here; however, a general description, provided by TMA, follows:

A collimated diode laser at 0.86 micron will be used as a source beam. Three or four silicon detectors will be used to monitor scatter at angles from  $10^\circ$  to  $70^\circ$  from specular (a longer wavelength source with Germanium detectors may also be used to extend the measurements to rougher surfaces). The data will be curve fitted for analysis and plotting using TMA's CAST analysis software package. The electronics will consist of a detector multiplexer, programmable lock-in amplifier, A/D converter, source modulator and power source. Signals from all of the reference detectors and the scatter detectors will be routed to the computer-controlled multiplexer boards which select the appropriate signals for the lock-in amplifier. The lock-in amplifier signals are transferred to the A/D converter and subsequently converted to digital signals for storage and later analysis.

The samples used with the scatterometer will mainly be of optical materials and coatings and will have optically smooth surfaces. The samples will be mounted as described on page 14 in the section on the microscope. Various samples will be positioned, one at a time, in front of the scatterometer, on the same scanning stage as is used for the microscope.

### Scanning Optical Microscope

Serial, visual observations of surfaces of materials during their exposure to the space environment in order to monitor their degradation over time is of interest to the space science and engineering community. Up to the present, only integrated exposure observations have been possible on samples retrieved from orbit after being exposed to space conditions. Images taken on the ground by the Scanning Electron Microscope (SEM) of Kapton specimens that had been exposed on the Space Shuttle (STS-8) have displayed an erosion morphology with features from sub-micron to a few microns in size. The exposure level of these samples was about  $3.5 \times 10^{20}$  O-atom/cm<sup>2</sup>, corresponding to about one week on orbit. ATOMS, on the other hand, will provide the opportunity to obtain periodic in situ observations of samples exposed on orbit for at least one year, by means of a remotely controlled microscope with an imaging and RF telemetry capability. In this manner, sample erosion morphology can be monitored as it forms in time.

At the early stages of this study, both Scanning Electron Microscopes (SEMs) and Scanning Optical Microscopes (SOMs), with resolutions of 0.5 micron, were investigated for purposes of in situ observation of various types of samples. The complexities and costs (\$2M to \$8M) of instruments with that resolution resulted in their elimination mid-way through the study. After further consideration of the problem, however, the conclusion was reached that the resolution requirement could be relaxed to 2 microns, without appreciably compromising the effectiveness of this instrument for space application. Under these circumstances, it was determined that a scanning optical microscope could be built in house from commercially available and off-the-shelf components at greatly reduced costs, as compared with the quotes received for the 0.5 micron instruments. A two-micron resolution will permit monitoring of specimens which have relatively rougher surfaces than those used with the scatterometer, as well as specimens composed of materials which cannot be used with the QCM instrument, such as composites.

In practice, even with a corrected objective, the 2 micron resolution could not be attained everywhere in the image plane of a conventional microscope. Other major problems are shallow depth of field and very small working distance. Through the use of scanning techniques, however, a considerable improvement can be achieved in the resolution and quality of the image with, theoretically, unlimited magnification and depth of field.

There are several forms of scanning optical microscopes. In each of them, one or more components are scanned, while the rest of the components are fixed. The one we have defined in this study is known as the confocal scanning optical microscope. The principle of operation of this microscope is illustrated in Figure 8. The light coming through a pinhole is focused to a diffraction-limited spot on the surface of the sample. A second lens is focused on the same spot to collect light from that spot and focus it on

a second pinhole in front of the detector. An image is built up by scanning the source and detector in synchronism, or by scanning only the object. The two lenses are said to be confocal, since both are focused on the same point. In reflection, one objective is used to focus the light on both object and detector. With this microscope, the resolution is improved at the expense of the field of view, while the latter is increased by lateral scanning. Effectively, the field of view and depth of field are as large as they need to be, limited only by the range of the lateral and axial scanning stages, respectively.

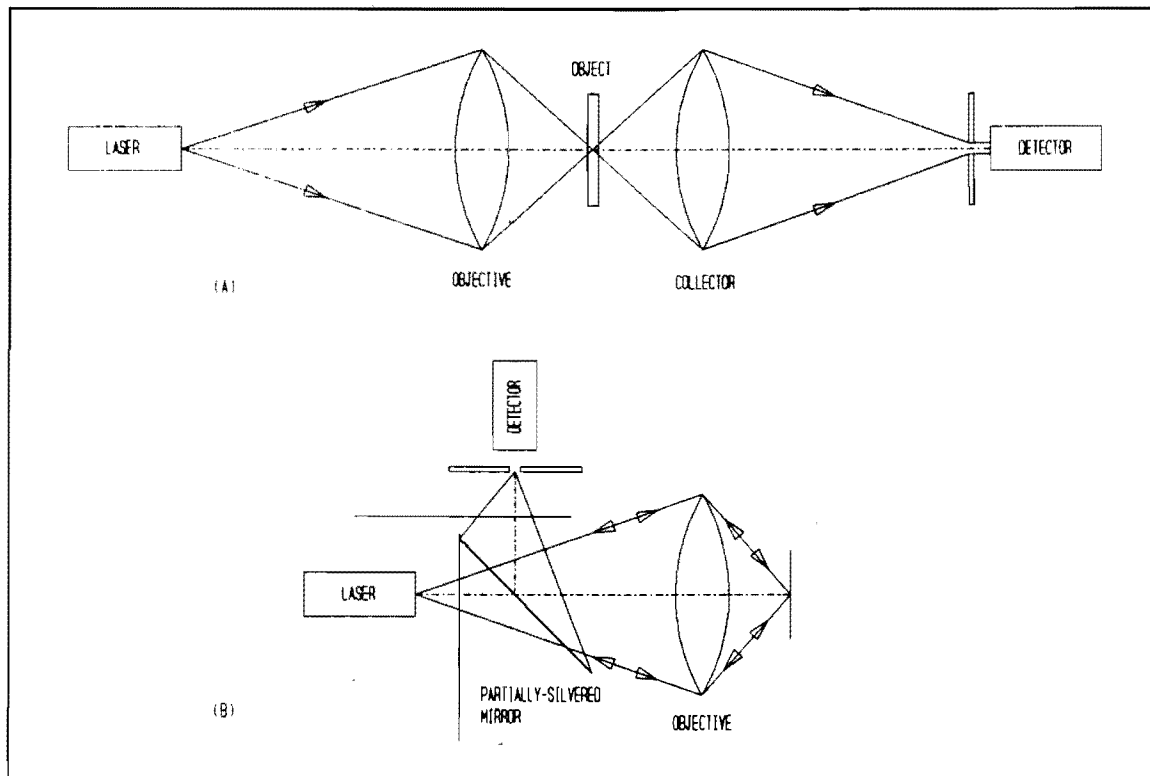


Figure 8: Confocal scanning optical microscope in (A) transmission and (B) reflection.

With this instrument, the image of the object is collected point by point, while the object is scanned in raster and in the axial direction. The data points will be transmitted to the ground where an image will be constructed and displayed for observation and analysis.

As mentioned above, two scanning techniques are possible. The first is to scan the focused light beam across a stationary object, and the second is to scan the object mechanically across a stationary spot. The advantage of the first is that the scanning can be very fast, so that many pictures can be built up per second; however, the design of the optics must be more complex, in order to eliminate the off-axis aberrations, and uniform resolution cannot be maintained over the entire image.

With the second scanning method, i.e., mechanically scanning the sample across a stationary spot, off-axis aberration requirements are relaxed, since the optical path will always be constant. In this case, the optics are much simpler, and uniform resolution is maintained through the entire image. Also, advantage can be taken of the relaxed off-axis aberration requirements to design a special lens, if desirable, with a higher numerical aperture and a longer working distance. We have selected the mechanical scanning technique for the in-space material imaging application.

With the confocal scanning microscope, the resolution is determined by the size of the light spot, and, therefore, by the power of the objective lens, as well as the wavelength and diameter of the light beam to be focused. Since a coherent light beam can be focused into a small spot much more easily than can an incoherent beam, a laser source of light is most appropriate for this instrument. For compactness and low power consumption, a laser diode will be used.

Laser diode collimating and focusing lenses with numerical aperture of about 0.4, are available commercially. These will focus a laser beam, of wavelength 0.67 micron, to a spot about 1.6 micron in diameter.

Figure 9 illustrates the optical design required to focus the laser spot on the sample. The laser source is a GaAlAs visible laser diode with wavelength 670-680 nm and optical power output of 3 mW (higher output powers, up to 10 mW, are also available if necessary). These diodes and their drive circuits are commercially available, in compact and rugged packages, from several well known companies such as Sony, Toshiba, RCA and Hitachi.

The output of the laser diode is a sharply divergent and asymmetrical, typically elliptical, cone of light. In order to couple efficiently to the optical system it is essential to collect, collimate and shape the beam first. As illustrated in Figure 9, L1 collimates and focuses the diode's output before shaping and expanding it with the anamorphic single-axis beam expander E1. The latter consists of two identical prisms mounted with respect to each other and to the incident beam in such a way as to introduce an anamorphic

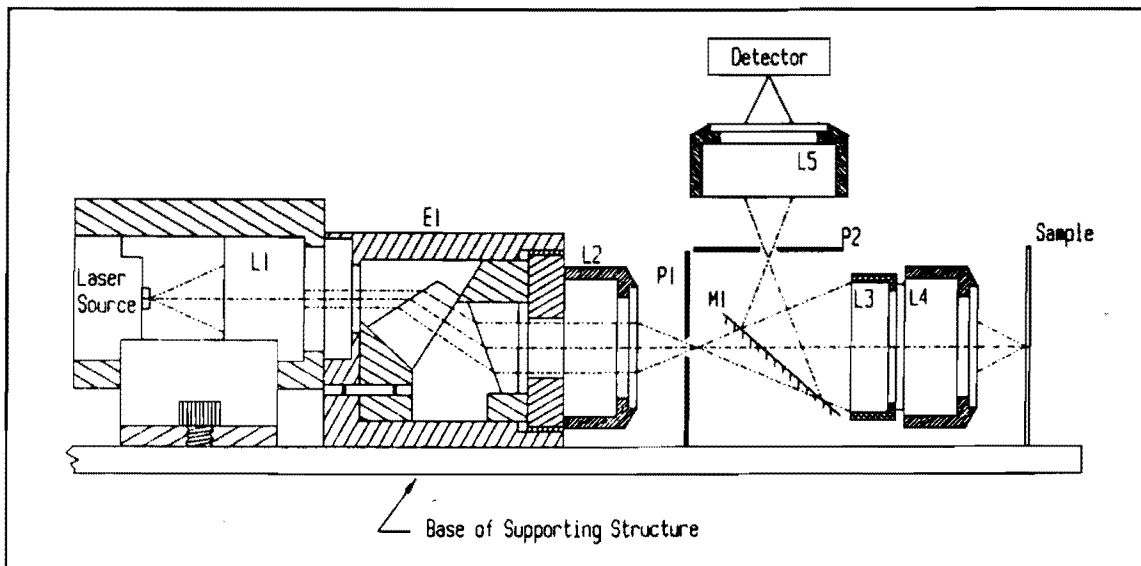


Figure 9: Optical component layout for scanning optical microscope.

expansion of the beam and, therefore, convert its shape to near-circular. The expanded beam will then pass through a spatial filter which consists of a focusing lens, L2, to focus the beam, and a pinhole, P1, to filter any noise in the beam. The focused beam will act as a point source at the pinhole P1. L3 and L4 are beam expander and focusing lenses which will expand, collimate and focus the beam on a small spot on the sample. The light reflected by the same spot on the sample will be focused on the detector, D, after being reflected by a partially silvered mirror, or a beam splitter, M1. The pinhole positioned in front of the detector is important to the quality of the image. If, during axial scanning, the sample is not accurately positioned at the focal point, the laser light, as illustrated in Figure 10, will illuminate a larger area on the sample. Consequently, the reflected light will not be properly focused on the detector and similarly will illuminate a larger area on it. The presence of the pinhole, however, will allow only a fraction of the reflected light to be detected. The maximum response of the detector will, therefore, be obtained only when the sample is accurately positioned in the focal plane. With this arrangement, the quality of the image is enhanced, and the resolution will be uniform throughout the image plane.

All the above optical components are commercially available with the proper coating at the required wavelength. The detector (D) is a silicon photo-diode with a fast response (rise time less than 50 ns) and linearity over a wide incident power range. Such detectors and their operating electronics are available in compact and rugged packages which comply with military/aerospace specifications.

The instrument and the sample mount will be positioned behind an opening in the satellite wall which faces

in the ram direction. A total of up to 16 specimens can be observed by the microscope. Pairs of specimens will be identically prepared from the same material. These samples, each 2 mm in width, will be glued, 1mm apart, on both sides of a 3 X 1 cm Aluminum strip, so that 8 of them will always be exposed to space, while the other 8, of exactly the same materials, will be protected and serve as reference samples. If composite materials are used, sample size may have to be larger, and fewer than 8 materials may be observed.

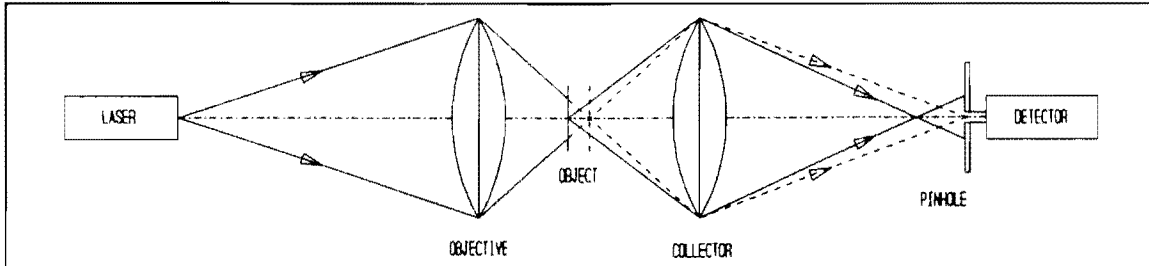


Figure 10: Importance of pinhole in obtaining sharp image.

Figure 11 illustrates the design of the sample mount. The sample strip will be connected to the shaft of a stepping motor, M, and will fit inside an opening in the plate, P. During observations this plate, which is at least twice the length of the sample strip, will act as a shutter for the exposure window. P will be rigidly attached to a 3-axis micro-positioning stage, ST, which is driven by piezoelectric inchworm motors. ST will provide scanning in the image plane, X-Y, and in the axial direction, Z, with a speed of up to 2 mm/sec and positioning accuracy of better than 0.1 micron.

The stage will provide up to 5 mm travel along both Y and Z axes, and up to 25 mm along the X-axis in order to scan all the samples. As shown in figure 11, an identical stage will accommodate the sample holder for the scatterometer measurements (see page 8).

At observation time, images will be obtained for the reference samples first. An image is obtained by raster scanning, in the X and Y directions, an area 100 microns X 100 microns on each sample, and by axial scanning in the Z direction to bring the sample to the focal point, where the photo-diode detects maximum intensity. The stepping motor will then rotate the sample strip to bring in the exposed specimens for observation. A clearance of at least 0.5 cm between the sample mount and the satellite wall will allow free rotation. The edges, E, of the sample strip, will touch a switch on the plate, P, to stop the motor after a rotation of exactly 180°. The reference samples will be exposed during the observation time. However, as explained later, it is a short exposure and will not affect our analysis.

The inchworm stage will be remotely controlled using a multi-axis, closed loop, inchworm controller with the proper interface to the computer on board the satellite.

With sensitive optical systems, such as the proposed microscope, precise adjustments and alignments are critical to the instrument performance. Thermal fluctuation and launching vibration are critical design problems which may destroy any pre-alignment. To avoid these problems, the optical components will be mounted in a special support structure, custom made to accommodate each of the system's components in its precise position. The structure will be made of strong, but lightweight, material to withstand the launch environment, and with near zero thermal coefficient to avoid any expansion or contraction due to thermal fluctuations.

The design will be thermally and mechanically analyzed, according to the expected thermal and mechanical environment during launch and flight. If necessary, as implied by these analyses, the design will be modified to minimize the effects of temperature fluctuation and mechanical vibrations.

As mentioned above, the image intensity shows a sharp maximum when the specimen is accurately positioned at the focal point. The distance scanned axially in the Z-axis is, therefore, related to the height of the surface of the sample at the observed point. During scanning, the stage position at the occurrence of the maximum will be measured and stored as surface profile information.

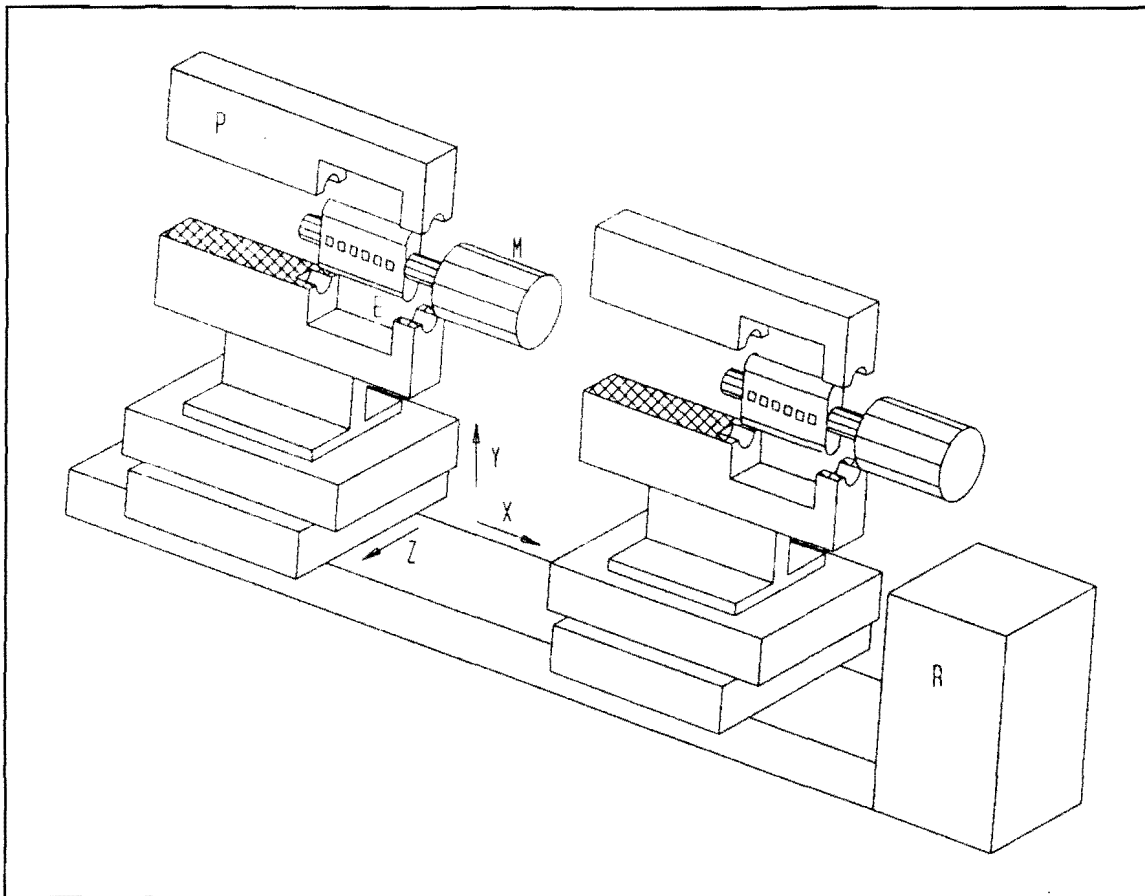


Figure 11: Sketch of sample mounting mechanism for microscope and scatterometer.

The performance of the scanning stage is vital to the quality of the image. For meaningful results, it is very important to scan the same area on each sample every observation time. The inchworm motors which drive the scanning stage have long life ( $>2 \times 10^{12}$  steps without motion degradation) and offer high resolution linear motion in a vacuum environment, with minimum mechanical backlash (noncumulative) of about 0.5 micron. Scanning, however, will be closed-loop controlled using encoders to provide constant monitoring of position and provide correction when necessary to maintain fixed positions. Patterns etched on the sample strip in the gaps between the samples will help in positioning each specimen. For more accurate scanning, the X, Y and Z positions of the stage will be measured along with the maximum intensity read by the detector at each image point. With the combined position and intensity information, an accurate image and profile will be constructed.

With a resolution of 2 microns, a maximum scanning step of 2 microns is required. However, a one micron step will produce a better image. The step for the axial scanning should always be at least half the lateral step, i.e. 0.5 micron. An area of 100 microns X 100 microns on the surface of the sample will be scanned, and, therefore, 10,000 image points will be obtained per sample. For each of the 10,000 image points observed per sample, there will be one intensity reading and three position (X, Y, and Z) readings; i.e., 40 kBytes of data are created per sample. For a maximum of 16 samples, a maximum total of 640 kBytes of data will be created during each observation. These data will be stored in the memory of the on-board computer until telemetered to a ground station. The images and profiles of the sample surfaces will then be reconstructed on the ground and viewed on a standard video monitor as 100 X 100 element pictures. These images can be enlarged, to practically any size, for proper observation and analysis, with a resolution equal to the spot size. Hard copies of these pictures can be generated by photographing the image displayed on the monitor.

### 3. SELECTION OF MATERIALS TO BE TESTED

The choice of materials to be tested in this initial small satellite program is critical. It is important to have a good match between the immediate and future needs of NASA and to insure a successful demonstration of the capabilities of small satellites. The priorities of the overall mission are:

**Proof of concept demonstration** -- It must be demonstrated that AO effects on materials in LEO can be quantified in a small satellite system. This priority mandates selection of materials known to degrade in LEO and with reasonably well-established rates of degradation, such as Kapton H-film, Mylar, carbon, osmium, silver, etc (see Leger et al. in Proceedings of NASA Workshop on Atomic Oxygen Effects, pg 6) [7].

**Satisfaction of NASA Short Term Needs** -- This mission also represents an opportunity to perform flight testing of recently developed AO-resistant materials and coatings under evaluation [8] for upcoming long duration NASA missions. These materials/coatings may also be under consideration primarily for use in thermal control and contamination control; thus, environmental resistance or stability of these materials is a major concern to NASA. Examples of such materials are Teflon, silicone-based coating materials (McGhann-NuSil cv-1144 series), or fluorosilicone coatings (CV-3530). The coating materials should be applied over a material, such as Kapton, with known degradation properties, in order to assess the durability of the coating, effects of pinholes or scratches, tendency to peel or flake when undercut, etc. Some consideration should be given to selection of optical materials, in particular, front-surface mirror materials for large space reflectors (metals) to exploit the BRDF instrument capabilities.

**Satisfaction of NASA Long Term Needs** -- The experiment package proposed for this mission will permit simultaneous real-time measurement of several material properties (mass loss rate, optical surface changes, thermal properties, mechanical properties). The need to develop a mechanistic model or understanding of AO attack and the possible synergism with solar radiation (thermal cycling, vacuum UV) is critical for development of new materials/coatings with exceptional environmental stability for long-term missions. There are some model polymeric systems which will permit mechanistic studies to be performed in situ, such as the fluorinated polystyrene (PS) series: pure PS, ring-only fluorinated PS, backbone (chain) fluorinated PS, and perfluorinated PS.

Exposure and response of such a series of polymers should provide very useful data in understanding the mechanism of attack and, perhaps more importantly, methods of stabilization of materials.

The finalized list of materials should be established at a later time, based on the availability of new materials, results from LDEF (hopefully) and thermal control materials/coatings in the above discussion. Some consideration for temperature measurement (via low thermal mass diode) should be addressed in the list of proposed experiments, since the behavior of thermal coatings is of considerable concern to NASA. Since there will be only a very limited number of slots for samples, a screening process will be required to establish the final materials selection. The JPL AO exposure facility will be available for use in this screening process, and a high priority will be given to accomplish such a task, if desired.

### 4. SPACECRAFT BUS DESCRIPTION

#### Spacecraft General Requirements

In order to preserve maximum flexibility in launch options, ATOMS has been configured to meet the STS Get Away Special canister constraints for small satellites. The GAS canister launch option constrains the weight of the satellite to less than 150 lbs and requires the spacecraft to fit within a right circular cylinder 19 inches in diameter and 18 inches in height. This is the most restrictive of all launch options available today. The Globesat GS-50 spacecraft bus has, therefore, been selected as the baseline for the project. If launch opportunities other than the STS arise (Scout, Pegasus, Delta, Atlas, Couestoga, AmRoc, etc.), the spacecraft and launch attachment can readily be adapted to any of these alternate platforms.

The standard GS-50 model comes with several supporting subsystems which will be appropriately modified to fit the ATOMS project.

The command and control computer, which is a Globesat standard product, will contain 4.5 megabytes



of memory to store the scientific data collected from the various instruments between transmissions to the ground.

The ATOMS power requirements will be provided by solar array panels, supplied by Solarex Corp., which will be mounted on the exterior of the bus structure, and by two 6-cell Gates "X" lead acid batteries.

Atoms communications will utilize a telemetry system, designed by Cynetics, Inc. for operation in a half-duplex mode in the experimental satellite band, between 137 and 138 MHz. At a communication rate of 9600 bps with a single ground station, the down-link capacity of the system is 17 Mb/day. This greatly exceeds the average data rate of 1 Mb/day generated by the experiments. The accumulated data will be transmitted during 1 or 2 spacecraft passes over the ground station.

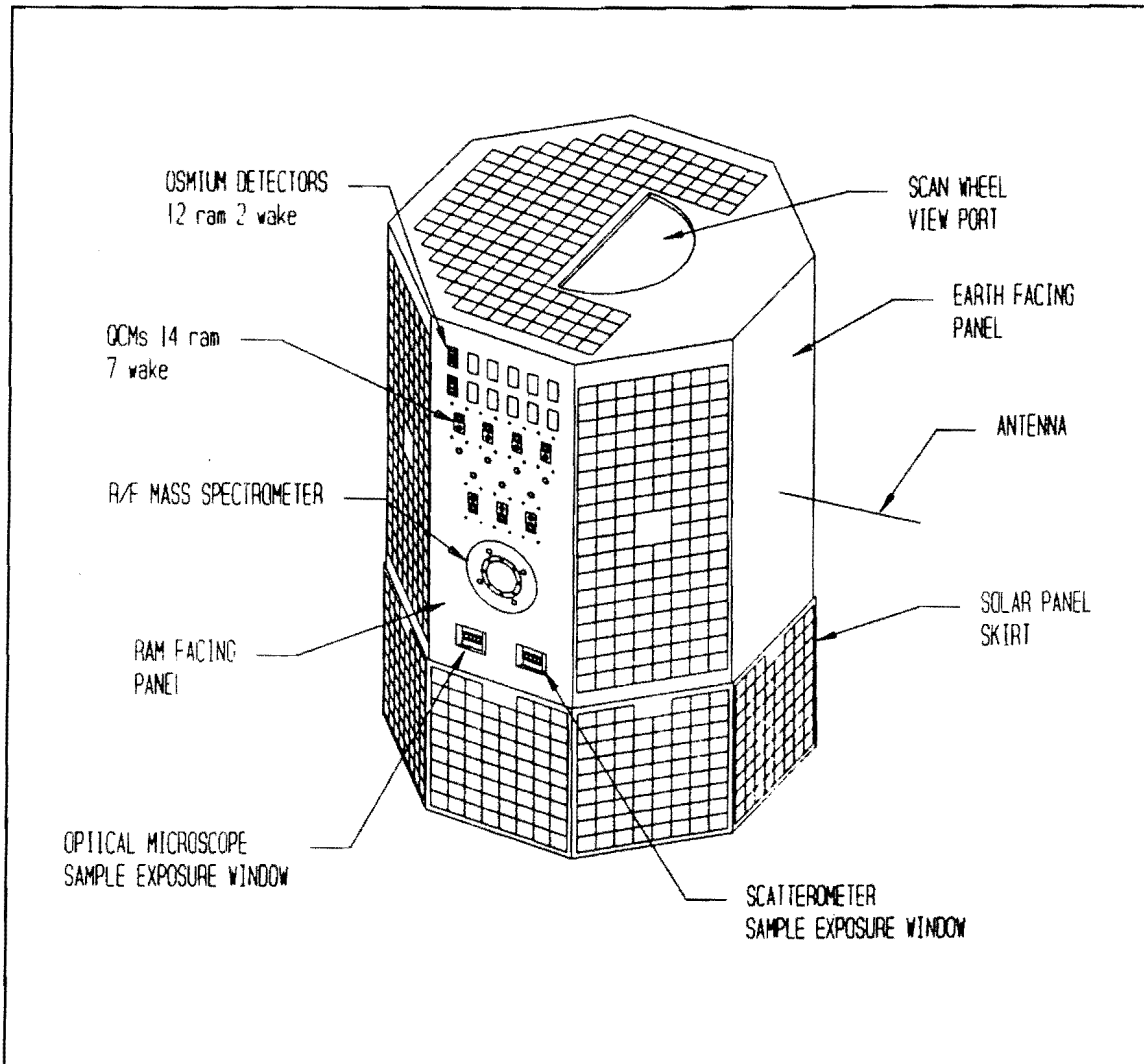


Figure 12: Satellite configuration (momentum wheel option) for thermal control calculations.

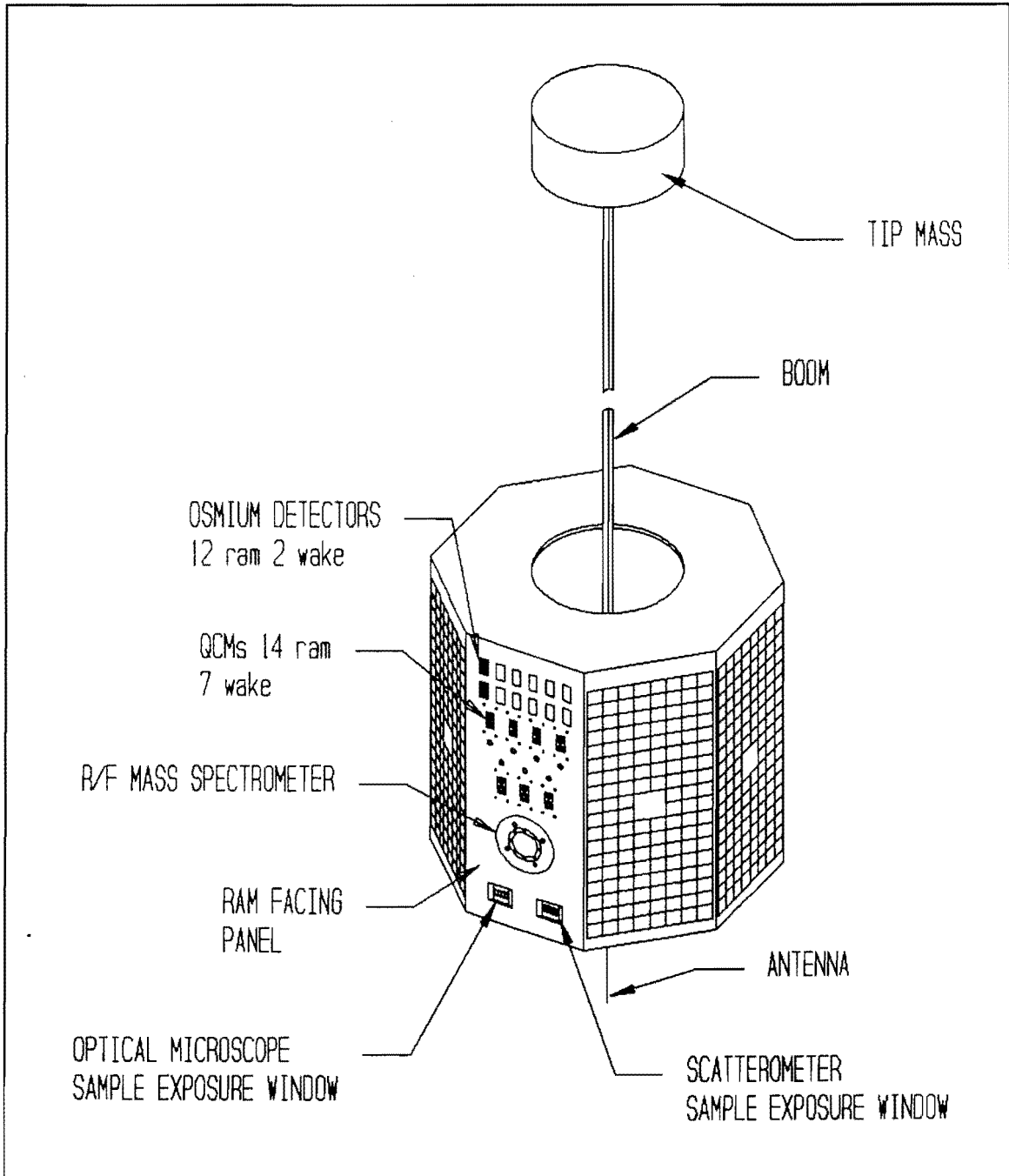


Figure 13: Satellite configuration (gravity gradient option) for thermal control calculations.

The mission requirements dictate the use of a **three-axis attitude determination and control system**. Two different systems have been identified as applicable to the satellite's mission. The first involves the use of a momentum wheel/horizon sensor, together with a magnetic torquing system (Figure 12). The second system involves the use of a gravity-gradient boom, coupled with an identical magnetic torquing system (Figure 13). The specification of a launch vehicle will largely determine the choice of the attitude system.

For a high altitude shuttle mission or an ELV launch opportunity, the gravity gradient attitude control system is appealing, because the primary stabilization is passive. Hence, it is not necessary to expend large amounts of energy for this purpose. Also, this system has the advantage of fewer moving parts than the momentum wheel option. In fact, the boom deployment mechanism is the only part which moves, and this is only a one-time movement.

The system will rely upon the gradient of the earth's gravitational field to induce torques on the spacecraft structure. These torques will tend to align the long axis of the spacecraft along the nadir vector. The spacecraft will be bistable; that is, either end could point towards the earth in a stable manner.

This method of stabilization requires the spacecraft's moments of inertia to be tailored such that two of the principal axes have large moments of inertia and the third principal axis has a much smaller moment of inertia. The moments of inertia are tailored by the deployment of a boom mechanism. The deployed boom is 9 meters long and has a 20 kg tip mass attached to it. The gravity gradient stabilization method is described in detail in a paper presented on the first annual conference on small satellites, Sept. 1987 [15].

The hardware for the gravity gradient attitude determination and control system is composed mainly of flight-proven devices. The boom deployment mechanism is a standard, off-the-shelf product of Wietzman, Inc, and has a space pedigree. The space-rated Torqrods are manufactured by the Ithaco Corporation and have been flown on numerous spacecraft. The magnetometer is supplied by the Humphrey Corporation and has an aerospace pedigree. The controller will be built using high-rel components with documented reliability. The software algorithms have been modeled extensively by the Ithaco Corporation.

For a shuttle launch option, a momentum wheel/horizon scanner together with a three-axis magnetometer and 3 Torqrods is the preferred option. This is because of the lower orbit altitudes typically attained by the shuttle. Our analysis has indicated that for typical shuttle orbit altitudes, 280 - 320 km, the gravity gradient system is not practical, because atmospheric drag forces begin to exert disturbing torques to the spacecraft structure which are of the same magnitude as the gravity gradient torques.

An Ithaco-built Scanwheel is employed, along with three orthogonally mounted torque rods and a magnetometer. The Scanwheel is a combination momentum wheel/horizon sensor and is mounted along the spacecraft's axis of cylindrical symmetry. The Torqrods are also built by Ithaco and are used to load and unload the Scanwheel angular momentum, as well as to precess the spin axis.

The magnetometer is used to sense the earth's geomagnetic field for determining the proper Torqrod usage. The Torqrods are mounted as far away as possible from the magnetometer. This reduces the effects of the retained magnetism in the Torqrods when making measurements with the magnetometer.

The combination momentum wheel/horizon scanner provides a gyroscopic stiffness which is used to keep the pitch axis of the spacecraft perpendicular to the orbit plane. The experiment face of the spacecraft is kept in the ram direction by making slight adjustments to the momentum wheel speed. The small adjustments to the wheel speed cause the spacecraft structure to react oppositely to the wheel speed change and conserve angular momentum.

The Torqrods and the magnetometer provide a capability for torquing the spacecraft structure. This capability is required for all phases of the ATOMS mission. This system can be expected to provide much better than +/- 5 degrees pointing accuracy. Accuracy of +/- 2.5 degrees is feasible. The hardware and software for the Scanwheel ACS are completely flight proven and have been used on many spacecraft including the HCMM and SAGE.

## REFERENCES

1. Leger, L.J., "Oxygen Atom Reaction with Shuttle Materials at Orbital Altitudes," NASA TM-58246, 1982.
2. Leger, L.J., Spiker, I.K., Kuminecz, J.F., Ballentine, T.J., and Visentine, J.T., "STS Flight 5 LEO Effects Experiment- Background Description and Thin Film Results," AIAA Paper 83-2631-CP, Shuttle Environment and Operations Meeting, Washington, D.C., Nov. 1983.
3. Visentine, J.T., Leger, L.J., Kuminecz, J.F., and Spiker, I.K., "STS-8 Atomic Oxygen Effects Experiment," AIAA Paper 85- 0415, 23rd Aerospace Sciences Meeting, Reno, Nev., Jan. 1985.
4. Visentine, J.T., and Potter, A.E., "In-Space Technology Development: Atomic Oxygen and Orbital Debris Effects," NASA TM-102154, 1989.
5. Clark, L.G., Kinard, W.H., Carter, D.J., and Jones, J.L., "The Long Duration Exposure Facility (LDEF) - Mission 1 Experiments," NASA SP-473, 1984.
6. Private communications, Visentine, J.L., NASA/JSC, Dubel, J., Sparta Corporation, Spring 1989.
7. "Proceedings of the NASA Workshop on Atomic Oxygen Effects", JPL Publication 87-14, June 1, 1987.
8. P.N. Peters, J.C. Gregory, and J. T. Swann, Applied Optics, 25(8), 1290, (1986).
9. J. M. Notley, Trans. Inst. Metal Finishing, vol. 50, 58, (1972).
10. Laher, R.R., and Megill, L.R., "Ablation of Materials in the Low-Earth Orbital Environment", Planetary and Space Science, Vol.36, pp. 1497-1508, (December 1988).
11. J.C. Stover, "Optical Scatter", Laser and Optronics, (August 1988).
12. J.C. Stover, S.A. Serati, C.H. Gillespie, "Calculation of Surface Statistics from Light Scatter", Optical Engineering, Vol. 23, No. 4, P. 406, (1984).
13. E.L. Church, M.A. Jenkinson, J.M. Zavaa, "Measurement of the Finish of Diamond-Turned Metal Surfaces by Differential Light Scattering", Optical Engineering, Vol. 16, No. 4, P. 360, (1977).
14. E.L. Church, "Fractal Surface Finish", Applied Optics, Vol. 27, No. 8, P. 1518, (1988).
15. Ali Siahpush and Andrew Sexton, "A Study for Semi-Passive Gravity Gradient Stabilization of Small Satellites", Proceeding of the First annual USU Conference on Small Satellites, Center for Space Engineering, Oct. 7-9, (1987).